



Analysis of network topology and deployment mode of 5G wireless access network

Zhiliang Liu ^{a,*}, Zengzhi Zou ^b

^a School of Information Engineering, Huanghuai University, Zhumadian 463000, China

^b Department of Computer Science, Zhumadian Agriculture School, Zhumadian 463000, China

ARTICLE INFO

Keywords:

5G wireless access network
Network architecture
Random deployment of cellular networks
Base station deployment
Cross-domain deployment

ABSTRACT

Aiming at the characteristics of high-density and random deployment of 5G cellular networks, through efficient network-level deployment methods, the network can quickly and efficiently adapt to large-scale dynamic changes in user traffic. Aiming at the need for 5G systems to meet the requirements of high-speed mobile environment communications, this paper deeply studies the factors that affect communication quality in mobile scenarios and their relationships. Based on this, around the content transmission and distribution of information, a 5G mobile communication network architecture based on content-centric network technology is proposed. To meet the deployment requirements of cross-domain VNF (Virtual Network Function) during the deployment phase, in order to solve the problem that the existing cross-domain deployment algorithms do not take into account node computing resources and link bandwidth resources, this paper proposes a DPSO-K (Discrete Particle Swarm Optimization—Kruskal) 5G cross-domain virtual network function deployment method. Compared with the traditional method, the overall cost is reduced, and the cost is least affected by the number of data fields. In different practical scenarios, the resource reduction gain of the strategy is evaluated. Simulation results verify the impact of different system parameters on the energy efficiency of the network. The results show that this method has obvious advantages in optimizing the energy spectrum efficiency of randomly deployed networks.

1. Introduction

With the rapid development of new technologies such as smart phones and the Internet of Things, the field of mobile communication technology is also undergoing unprecedented changes [1]. From the perspective of the number of users and the total amount of services, mobile communications will continue to maintain a high-speed development trend [2,3]. The rapidly growing demand has brought huge opportunities and challenges to the development of mobile communication network technology, and has caused a wave of R & D on new services, new technologies, new standards and new products in the academic and industrial circles. In this environment, 5G has become a new hotspot leading the development of communication technology and has broad application prospects [4]. With the rapid development of wireless mobile device technology and the widespread popularity of mobile Internet services, the high-density deployment of wireless access points has become the core method for providing ubiquitous high-rate user access and greatly improving the utilization of network resources.

With the evolution of mobile services from traditional voice services to mobile data services, ubiquitous high-speed wireless services have become a major task facing next-generation cellular networks [5]. As

a result, mobile operators are busy deploying a large number of base stations to meet the above challenges [6]. There is no doubt that improving the spatial reuse of frequency resources and reducing the distance between mobile users and base stations can achieve higher system capacity [7,8]. However, more cells will inevitably lead to a large increase in energy consumption, which will cause corresponding environmental and economic problems. As we all know, the fifth generation mobile communication network must not only achieve a substantial increase in system capacity and enhance the user experience, but also meet the efficient use of energy resources. Therefore, achieving higher network energy efficiency and capacity are key performance indicators for next-generation network deployment and planning. Up to now, a large amount of literature has been working to reduce the energy consumption of the network and improve the energy efficiency of the network, and has given relevant conclusions [9–11]. It is worth noting that nearly 75% of the energy consumption comes from the base station [12]. And, in a base station, 70% of the energy comes from the power amplifier, cooling device, etc. of the base station. Therefore, the energy consumption of the network mainly depends on the density of the base station and the operation mode of the base station. Obviously, the deployment of base stations must meet the greatest business requirements [13,14]. However, when the network load is reduced, many

* Corresponding author.

E-mail address: li2920ning@126.com (Z. Liu).

base stations will be in a semi-idle state and consume a lot of energy to maintain network coverage [15]. Therefore, improving the utilization efficiency of energy resources should start with the business load of the time-varying space. In related research on VNF (Virtual Network Function) cross-domain deployment, the connection relationship between VNFs is usually regarded as a virtual network with static resource requirements, and the static cross-domain VNF deployment of network slices is transformed into a cross-domain virtual network mapping [16]. The existing cross-domain virtual network mapping mainly includes distributed and centralized methods [17]. Among them, the distributed method cannot obtain the best cross-domain virtual network mapping solution due to lack of network-wide information. Centralized cross-domain virtual network mapping is generally divided into two stages: virtual network partitioning and virtual subnet mapping. Related scholars have proposed a heuristic algorithm based on the greedy approach, but this method does not take into account the node computing resources and link bandwidth [18]. Researchers use the meta-heuristic algorithm to segment virtual network requests based on the price of border nodes and inter-domain links in a multi-domain network, but this method has a limited reduction in node and link resource overhead [19]. Relevant scholars have designed a virtual network partition method based on the node information by analyzing the information of the boundary nodes, but this method faces the problems of too long algorithm execution time and high complexity [20]. Relevant scholars have given a topology constraint mechanism to achieve efficient cellular base station deployment technology, which can increase energy consumption by more than 40% [21]. In the deployment strategy of the joint macro base station and small base station, the influence of the density of the macro base station and the density of the small base station on the coverage probability is studied [22]. Some base station deployment strategies based on probability statistics techniques, such as meta-heuristic methods and simulated annealing algorithms, are used [23]. According to different user distribution scenarios, the number and location of required base stations are optimized by scholars [24]. In practice, long-term user information statistics are important for the use of cellular base station deployment technology.

Starting from the concept of the content-centric network, the network architecture is designed around the transmission and distribution of information content. Based on this, the improvement of the communication performance of mobile nodes is studied, and the frequent switching of mobile nodes with the content-centric network architecture in the high-speed mobile scenario is studied. This paper proposes a 5G mobile communication network architecture based on the content-centric network, and studies the communication performance of the 5G architecture based on the content-centric network. With the goal of optimizing resource overhead, the static deployment problem of cross-domain VNFs is translated into cross-domain virtual network mapping, and the solution of cross-domain virtual network mapping is analyzed. We propose a cross-domain VNF static deployment solution to reduce the mapping resource overhead. An accurate model was established to solve the energy spectral efficiency of randomly deployed cellular networks, and an accurate energy spectral expression was derived. It is an expression of base station density, load-aware density, average user rate requirements, and other network parameters. At the same time, an optimal base station deployment strategy was designed to maximize the energy spectrum efficiency of the network while taking outage probability as a constraint. The simulation results illustrate the superiority of the proposed model.

The rest of this paper is organized as follows. Section 2 analyzes the 5G mobile communication network architecture based on the content-centric network. Section 3 studies the deployment of 5G cross-domain virtual network functions based on DPSO-K (Discrete Particle Swarm Optimization—Kruskal). Section 4 studies the deployment of traffic-aware high-energy spectrum-efficient base stations in randomly deployed cellular networks. Section 5 summarizes the full text and points out future research direction.

2. 5G mobile communication network architecture based on content-centric network

2.1. Content center network architecture

Unlike IP (Internet Protocol) networks, content-centric networks are centered on information content, relying on named data for transmission over the network, and no longer focus on user address information. The data packets of the content-centric network are marked with unique names, changing the original encapsulation structure and addressing mode. Compared with the current architecture of the Internet, content-centric networks can better solve communication problems. The distributed content server network structure is shown in Fig. 1.

The architecture of the content center network and the IP network both adopt a 7-layer architecture, and both retain the “hourglass model”. The purpose of the lower-layer protocol design is to adapt to the underlying physical link, and the purpose of the upper-layer protocol design is to correlate. application. However, the IP network architecture is based on the IP protocol and the content-centric network is based on the content block protocol. Therefore, the architecture of the content-centric network and the IP network mainly distinguishes between the forwarding strategy and its own security, and multiple connection methods are adopted at the same time, such as connection with Ethernet, mobile communication network, Bluetooth, etc.

Unlike IP networks, there is no independent transport layer in the architecture of the content-centric network. Instead, it relies on the forwarding strategy layer to implement the functions of the transport layer and network layer of the IP network at the same time. Therefore, the architecture of the content-centric network can achieve flexible and reliable data transmission. In IP networks, routers direct the forwarding of packets based on the IP address prefix, and a packet can only be used by one user; content-centric networks build routing tables based on content name prefixes, and routers in content-centric networks have caches. One data packet can be shared by multiple users. Even if the network link is interrupted, users can obtain information from nearby routers to reduce the interruption delay time and maintain normal communication. The architecture of the content-centric network is based on content security. It does not rely on the security of the transmission channel. It encrypts the content transmitted on the network, that is, all content must be verified by digital signatures. Therefore, many IP networks can be avoided.

Therefore, the architecture of the content-centric network is flexible and reliable, and provides conditions for implementing a series of functions such as fast retrieval, intelligent forwarding, and efficient content caching.

(1) Content center network data packet structure

The communication process of the content-centric network is driven by the data requester and is realized by exchanging Interest packets and data packets. The data requester encapsulates the name of the content it wants to get into the Interest packet and forwards it to the data provider. After receiving the Interest packet, the data provider encapsulates the content name, the requested content, and the information of the data provider into the data packet, and then sends the data packet back to the data requester. If the requested content is stored in the nodes along the way, the corresponding data packet will be returned to the data requester directly without visiting the data provider. Data contains the same name as the Interest packet, and the transmission process of the data packet is driven by the Interest packet, that is, a data packet can only match one Interest packet request, but a data packet can simultaneously meet multiple users with the same requirements. It can be seen that the content center network has the characteristics of load balancing and saving traffic.

Because the architecture of the content-centric network fully considers the efficiency and security of data communication, the Interest package and data package contain some additional information in addition to some necessary information. For example, adding Nonce

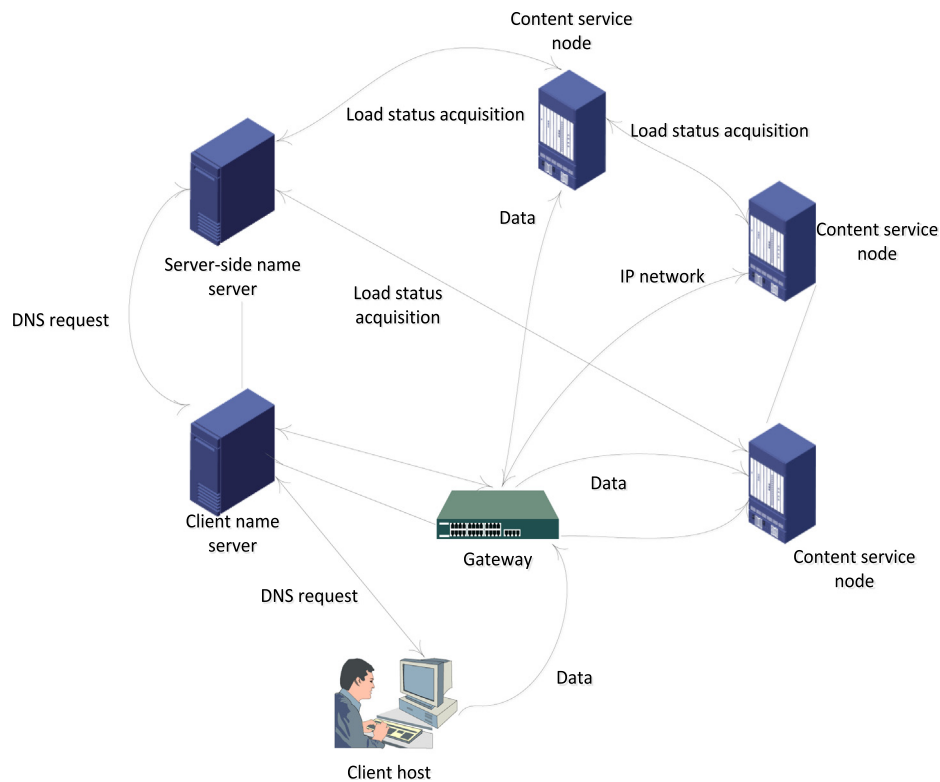


Fig. 1. Schematic diagram of distributed content server network structure.

to the Interest package ensures that there are no duplicate Interest packets flowing in the network to avoid wasting network bandwidth. Adding a data signature to the data package can verify the exact identity of the data provider, thereby ensuring the security of network communications. In addition, other information can be added to the Interest and data packages as needed.

(2) Content center network forwarding and routing mechanism

The network nodes of the content center network include three data structures, namely PIT (Pending Interest Table), FIB (Forwarding Information Base), and CS (Content Store). The PIT stores all the Interest packet forwarding information that is forwarded by the router but has not yet received a data packet response. Each PIT entry records the requested content name and the port number when the Interest packet enters the router, which is convenient for returning the corresponding data packet. The FIB of the content-centric network is similar to the routing table in the IP network. It provides path information for packet forwarding. However, IP networks allow only one port to be used to forward data packets, while content-centric networks allow multiple ports to be used to forward data packets simultaneously. In addition, routers in the IP network construct routing tables based on the address prefix information, while FIB tables in the content-centric network guide the forwarding of Interest packets based on the prefix of the content name. CS is used to store the recently applied Data packets. Since the Data packets of the content center network no longer pay attention to address information, it can satisfy multiple Interest packets with the same request, saving bandwidth and traffic for network communication. The schematic diagram of the route forwarding process is shown in Fig. 2.

When the Interest packet arrives at a certain port on the router, it must first be retrieved in CS based on the content name according to the longest prefix matching principle to check whether there is a corresponding data packet. If retrieved contains the corresponding data packet, the data packet is directly passed back to the user, and then the Interest packet is discarded, otherwise the PIT is retrieved. If the PIT contains an entry that matches the requested content, it means that

the same application has been received before and the corresponding Interest packet has been forwarded, but there is no response from the data packet. Therefore, the information of the Interest packet is added to the corresponding PIT entry, and then the Interest packet is discarded. If there is no matching content in CS and PIT, it means that this router received the Interest packet containing the content name for the first time, then a corresponding entry is established in the PIT, and according to the forwarding information of the FIB table, Interest packets are forwarded to the data provider.

2.2. Research on 5G mobile communication network architecture based on content-centric network

In order to meet the challenges that 5G application requirements and technological scenarios pose to the network, 5G networks need technical innovations in both the basic network platform and the network architecture. The 5G network introduces the Internet and NFV (Network Function Virtualization) to design and implement a new basic network platform based on general hardware, thereby solving the problems of high cost, poor compatibility, weak dynamic resource allocation capabilities, and long service deployment cycles of existing platforms. In terms of network architecture, a new network architecture was developed and designed using technologies based on control and forwarding separation and control function reconfiguration to improve the overall access performance of the access network and meet the needs of complex 5G scenarios.

Based on the characteristics of the 5G core network that needs to support various services with low latency, low transmission interference time, high reliability, large capacity, and high speed, the content-centric network architecture has advantages. The introduction of a content-centric network will better meet network performance quality requirements. Therefore, this paper proposes a 5G architecture based on a content-centric network. Considering the compatibility with the original network architecture, the network architecture is divided into four parts: application layer, network layer, data link layer and

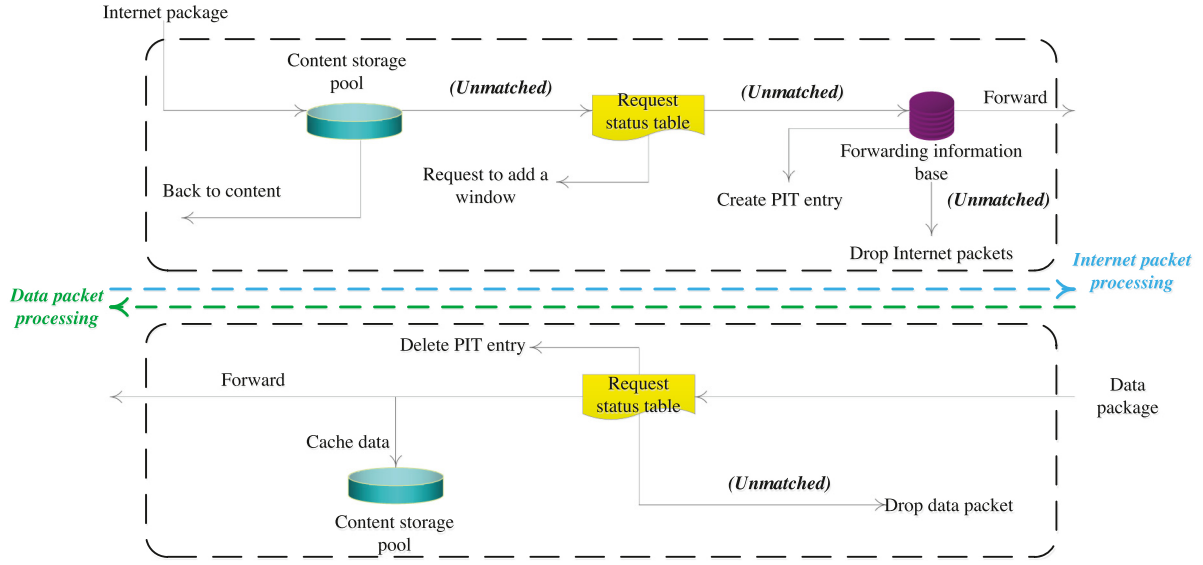


Fig. 2. Schematic diagram of route forwarding.

physical layer. Among them, the application layer, data link layer, and physical layer use the same protocol as the existing TCP/IP-based packet data communication mode in the existing IP network; the content-centric network protocol is used in the network layer. That is, the application layer data packets enter the network layer after being encapsulated, and the content-centric network protocol is used in the network layer. Therefore, based on the original packet data communication mode based on the TCP/IP protocol, by embedding the network layer based on the content-centric network architecture, the purpose of changing the network layer architecture is achieved so that it can provide better service quality. When a user sends an Interest request for a certain content, the data transmission process is as follows:

- (1) The content name of the Interest request is encapsulated in the Interest packet and forwarded to the content center network;
- (2) When the router in the network receives the Interest packet, it will process the Interest request according to the content-centric network protocol forwarding strategy and workflow;
- (3) If the Interest request is different from the previous request, it will forward the corresponding Interest packet to the data source through Ethernet or other connection methods;
- (4) The data source encapsulates the corresponding content into the data package, and returns the data package to the user in the same way as when the Interest package came.

3. DPSO-K-based 5G cross-domain virtual network function deployment

3.1. Establishment of cross-domain virtual network mapping model

After defining the related concepts of the underlying physical resource network and virtual network, we use the following formula to represent the concept of virtual network mapping:

$$VNE: G_v = (N_v, E_v) \rightarrow G_s = (N_s, E_s) \quad (1)$$

The optimization goal of this section is to choose a cross-domain virtual network mapping scheme that maximizes overall revenue and minimizes overall overhead to improve resource utilization. In order to consider node computing resources and link bandwidth resources as a whole, the cost of cross-domain virtual network mapping is defined as the total cost of node computing and link bandwidth. The specific formula is as follows:

$$Cost(G^v) = (1 - \alpha) \sum_{e^v \in E^v} be^v + \alpha \sum_{n^v \in N^v} cn^v \quad (2)$$

Among them, α is an adjustment coefficient, which can balance node overhead and link overhead.

During the execution of the mapping algorithm, the available computing resources on all nodes of the physical network are as follows:

$$R(n^s) = \sum_{n_s \in N_s} c(n_s) - \sum_{n_v \in M_v^c} c(n_v) \quad (3)$$

That is, the computing resources on all physical network nodes minus the computing resources that have been allocated. Among them, M_v represents the virtual node that has been mapped and deployed.

Similarly, during the execution of the mapping algorithm, the remaining available bandwidth resources are expressed as:

$$R(e^s) = \sum_{e_s \in E_s} be_s - \sum_{e_v \in M_v^e} be_v \quad (4)$$

The mapping process is to project the virtual network on the underlying physical network. Therefore, in the mapping process of the virtual network, the remaining resources of the underlying network must be greater than the resource requirements of the virtual network, which is characterized as:

$$\begin{cases} c(n^v) < R_N(M_N(n^v)) \\ b(e^v) < R_E(M_E(e^v)) \end{cases} \quad (5)$$

In addition, the computing resources on the physical nodes must be greater than the computing resource requirements of the virtual nodes, and the bandwidth resources between any physical nodes must also be greater than the bandwidth resource requirements between the virtual nodes, which can be characterized as:

$$\begin{cases} b(n_v^i, n_v^j) < b(n_N^i, n_N^j) \\ c(n_v^i) < c(n_N^i) \end{cases} \quad (6)$$

Due to the special attributes of 5G services and the possible localization and differential deployment of various VNFs in the network, location constraints must be added when mapping virtual nodes, which is characterized by:

$$Loc(n_N, n_v) = \begin{cases} 0 & \text{Not deployable} \\ 1 & \text{Deployable} \end{cases} \quad (7)$$

3.2. Interdomain partial mapping algorithm

The main purpose of inter-domain mapping is to realize the division of virtual networks and determine the boundary nodes and

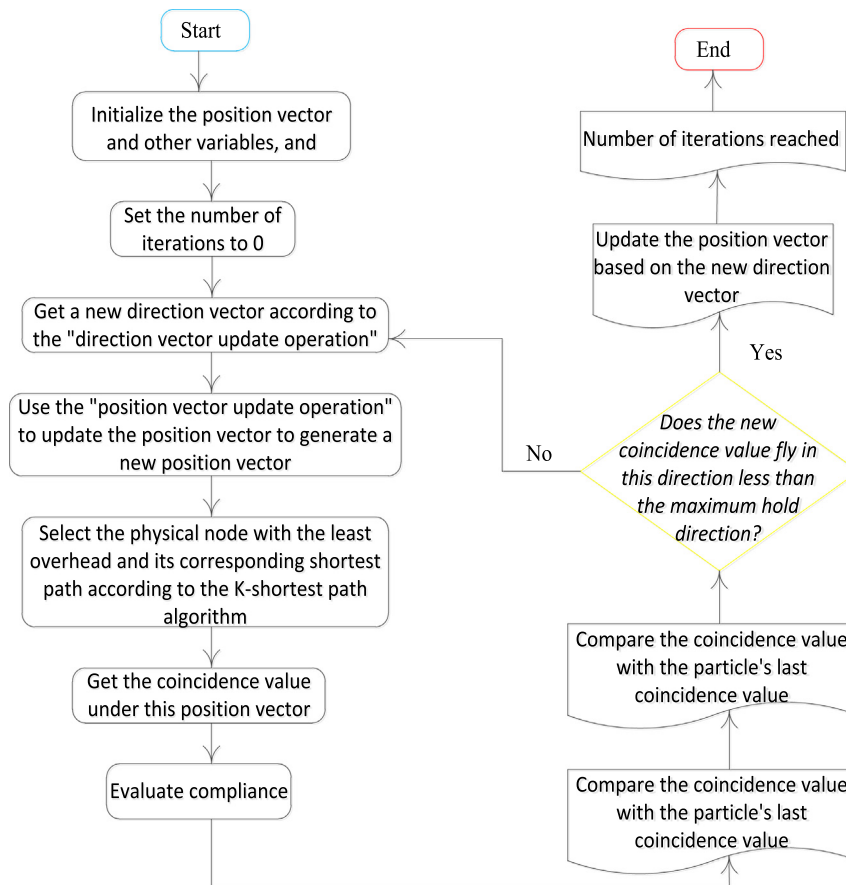


Fig. 3. Iterative process of discrete particle swarm algorithm.

inter-domain links. For the optimization of inter-domain link cost, a meta-heuristic algorithm is usually used. The goal is to find an approximate optimal solution to the problem in an acceptable time. This chapter takes the minimum link bandwidth overhead required for inter-domain communication as the goal, and uses an optimized discrete particle swarm algorithm to complete the inter-domain mapping and realize the division of virtual networks.

The main purpose of the inter-domain virtual network mapping is to achieve the division of virtual subnets, that is, to select appropriate forwarding nodes and inter-domain routing strategies, and thereby minimize cross-domain communication overhead. Communication between autonomous domains passes through inter-domain routing and forwarding nodes (that is, anchor points). When this node is selected across the entire network, the two physical nodes with the smallest link bandwidth resources are deployed first. This node acts as a cross-domain forwarding node to implement the deployment of inter-domain communication links. Therefore, the inter-domain link bandwidth and routing hops based on the node can be used as optimization goals to refine and disassemble the objective function formula of the cross-domain virtual network mapping model, and formulate the compliance function in the inter-domain mapping section as follows:

$$f = \sum_{(u,v) \in L_V} k \cdot BW(u,v) \cdot LEN(u,v) \quad (8)$$

The coincidence value of the interdomain coincidence function can be used as a criterion for measuring the excellent interdomain mapping. In the above conformance function, $LEN(u, v)$ refers to the two anchor points (u, v) . $BW(u, v)$ is the link bandwidth between any two anchor points; k is the adjustment factor for the link bandwidth. To meet the needs of intra-domain links, adjustment factors need to be introduced to adjust the compliance value.

Optimizing discrete particle swarm optimization is a multi-solution iterative process. The basic principle is to gradually iterate through the coordination and cooperation of particle swarms and resource interactions, and determine the optimal solution. Iterative process of discrete particle swarm algorithm as shown in Fig. 3. The parameter position vector is changed by parameter operation, that is, the value of each component is re-determined. The virtual node re-selects the physical node to match, and the location update operation is performed through multiple direction adjustment operations.

3.3. Experimental results and analysis

We run all simulation experiments on a computer with a 3.4 Ghz Intel Core i7 processor and 8 Gb RAM. All algorithms are implemented using Matlab, and the GT-ITM software is used to establish a virtual network topology and a physical network topology, respectively.

The DPSO-K algorithm proposed in this paper is compared with a matching algorithm based on iterative search (referred to as HTF) and a minimum cost algorithm based on binary integer programming (referred to as MC-VNM). In the simulation process, the value range of the number of virtual network nodes is set to [0–60], and the balance adjustment factor of node overhead and link overhead is set at the same time. We analyze and compare the total cost, request acceptance rate, and algorithm running time of 60 virtual network cross-domain mappings.

(1) Mapping overhead simulation

Fig. 4 is a comparison of the overall mapping overhead of the three algorithms with different numbers of virtual nodes. The algorithm takes the average of multiple experiments. As can be seen from the figure, the DPSO-K algorithm reduces the overall mapping overhead by considering the node resources and link resources and using the

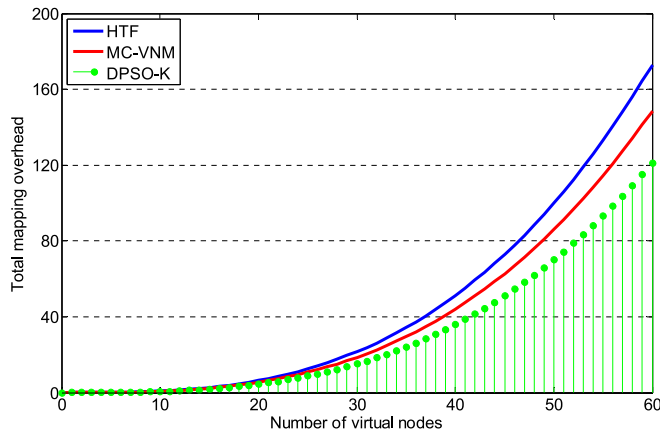


Fig. 4. Comparison of the overall mapping overhead of the DPSO-K algorithm.

discrete particle swarm algorithm to optimize. Compared with the other two methods, it can be reduced by an average of 5% in the current experimental environment. At the same time, it can be seen that with the increase of the number of virtual nodes, the increase rate of the overall mapping overhead of this algorithm is the lowest, which is suitable for large-scale network environments. In addition, as the number of nodes increases, the growth rate of overall overhead will slow down. This is because the resource requirements of the virtual nodes and the resource provision capabilities of the physical nodes are evenly distributed during the simulation process. The situation where the resources of the physical node cannot meet the demand is a service denial that is generated. This indicator can be measured by the request acceptance rate.

Fig. 5 shows the impact of the number of different data domains (physical subdomains) on the overall mapping overhead of the three algorithms. In order to verify the performance of the algorithm, while maintaining the node and resource information of the virtual network and physical network, only the number of data domains of the physical network is changed (5, 10, 15, 20 respectively). It can be seen that as the number of data domains increases, the overall mapping of each algorithm will gradually increase, but the overall overhead of the proposed algorithm increases relatively little (see Fig. 6).

(2) Comparison of request acceptance rate

In order to compare the request acceptance rate, the maximum number of virtual nodes is increased to 120, and cross-domain virtual network mapping is performed respectively in order. As can be seen from the figure, this algorithm uses the inter-domain mapping to achieve the maximum optimization of physical resources. By averaging multiple experiments, the average request acceptance rate of this algorithm is 94%, which is superior to two traditional cross-domain mapping algorithms.

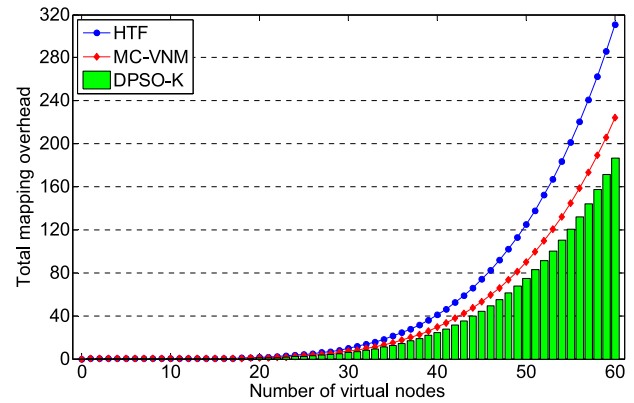
(3) Algorithm running time comparison

From the experimental data in Fig. 7, it can be seen that although the DPSO-K algorithm can reduce the overhead, the algorithm takes a long time to run. This is because the resource quotation is introduced in the part mapping based on the particle swarm, which leads to an increase in algorithm complexity. However, the rise in computing time is still in the same order of magnitude, and additional time overhead is acceptable in practical applications.

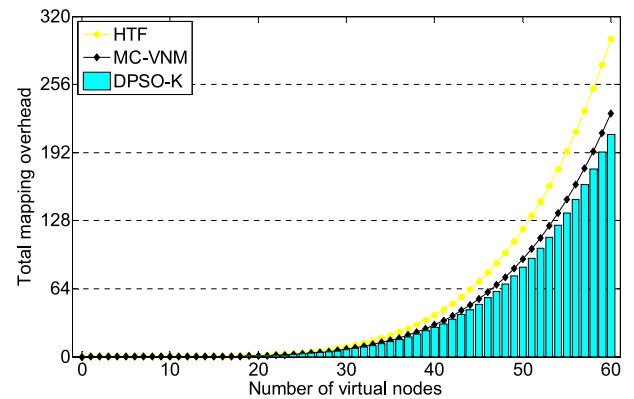
4. Random deployment of traffic-aware high-energy spectrum-efficient base station deployment in cellular networks

4.1. Network deployment model

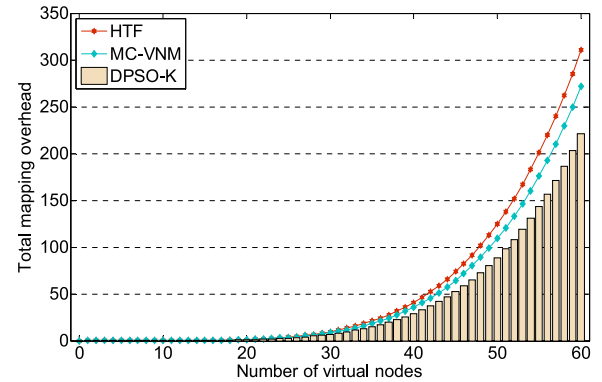
A large number of base stations are randomly distributed in the European-style plane R^2 , and their laws obey the spatial Poisson point



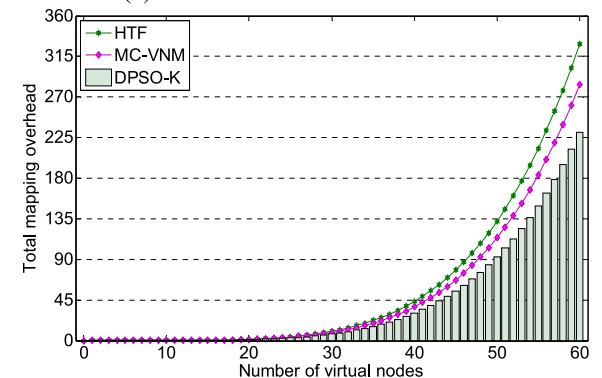
(a) The number of data fields is 5



(b) The number of data fields is 10



(c) The number of data fields is 15



(d) The number of data fields is 20

Fig. 5. Effect of the number of different data domains on the overall mapping overhead.

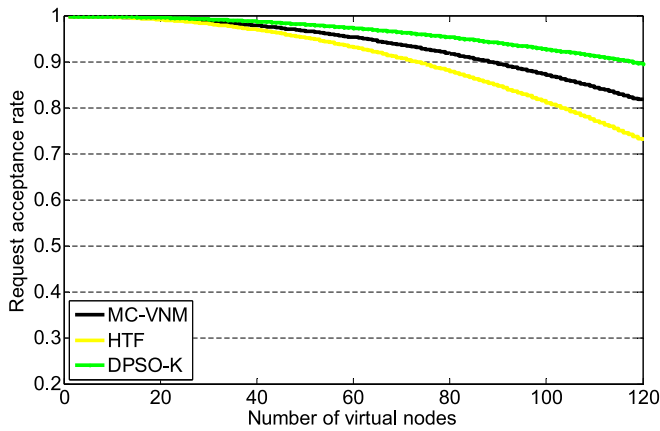


Fig. 6. Comparison of request acceptance rates of three algorithms.

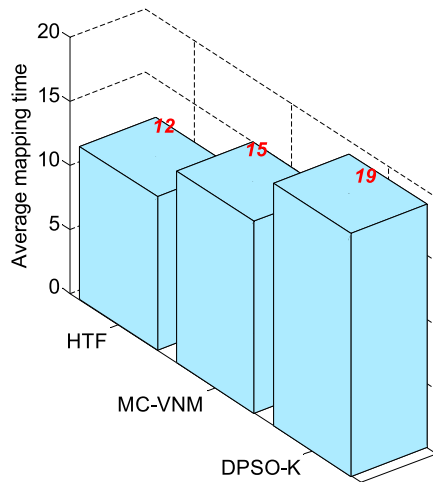


Fig. 7. Average mapping time comparison chart of three kinds of algorithms.

distribution. $\Psi_b = \{b_i, i = 0, 1, 2, \dots\}$ is used to represent the user set, and the distribution density is the base station density. The set Ψ_b of the base stations in the plane forms the Voronoi spatial distribution model, where V_i represents the coverage area of the base station b_i . Similarly, we use $\Psi_u = \{u_k, k = 0, 1, 2, \dots\}$ to represent the set of users in the plane, and the users obey the spatial Poisson point distribution in the plane. Any user u_k is connected to its nearest base station. Therefore, in the network model, the locations of base stations and users conform to two independent Poisson point distributions. When the average user rate is required, the spatial service load distribution density is equivalent to the user density. Therefore, the user density is used to represent the spatial load distribution density. An actual network scenario will be described by choosing a reasonable distribution density of users and base stations. For example, the base station density is 5×10^{-6} BS/m², and the load distribution density is 4×10^{-4} users/m². This scenario corresponds to a cellular network with an average cell radius of 250 m, and each cell accommodates an average of 80 users. In general, considering the total number of resource blocks in a cell, the user density/base station density ≤ 80 needs to be guaranteed. It is also assumed that the base station density 2×10^{-6} BS/m² is established. In other words, the average cell radius in the network model is no greater than 400 m. Another advantage of using Poisson point distribution is that the new network still conforms to the spatial Poisson point distribution when some base stations are closed or turned on.

In the downlink transmission of signals, both large-scale and small-scale fading are considered. Among them, the path loss can be expressed as:

$$L_\alpha(r) = cr^{-\alpha} \quad (9)$$

Among them, $c > 0$ is a constant and greater than 0, α represents a path loss factor, and r represents a distance between a user and a base station. At the same time, sharp fast fading is considered. The aggregate interference at user $u_{i,j}$ comes from the base station set $\Psi_b \setminus b_i$. The transmission power of the interfering base station set $\Psi_b \setminus b_i$ is the maximum value P_{\max} . Without special interpretation, the effect of channel noise is ignored, because in the model, the intensity of the interference is much greater than the noise. For any user $u_{i,j} \in \Psi_u$, i located in cell V_i , the received signal strength is:

$$P_{i,j}^{Rx} = P_{i,j} h_{i,j}^i \cdot L_\alpha(\|u_{i,j} - b_i\|) \quad (10)$$

At the same time, the corresponding received interference power is:

$$I_{\Psi_b/b_i} = \sum_{b_k \in \Psi_b/b_i} h_{k,j}^i \frac{P_{\max}}{N_i} L_\alpha(\|u_{i,j} - b_k\|) \quad (11)$$

$\|u_{i,j} - b_k\|$ represents the distance between the user $u_{i,j}$ and the base station b_k , and $h_{k,j}^i$ represents the fast fading channel gain between the user $u_{i,j}$ and the base station b_k , which meets the $h_{k,j}^i \sim \exp(1)$. Here, the channel gain is normalized to one.

4.2. Simulation and numerical results

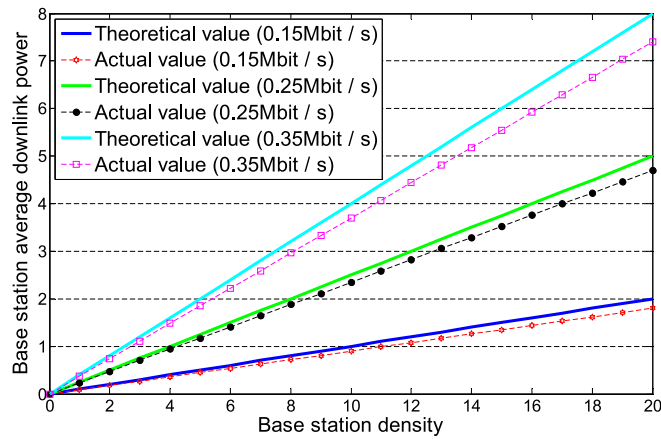
In Fig. 8(a), the average downlink transmission power of the base station b_i is depicted as a function of user density, given the cell coverage area $A_i = \pi \cdot 250^2$ m², B (base station system bandwidth) = 20 MHz. At the same time, Fig. 8(b) depicts the average downlink transmission power as a function of base station density, given user density = 10^{-4} user/m² and $B = 20$ MHz. It is found that the average downlink transmission power increases exponentially as the user density increases. As the base station density increases, the average downlink transmission power decreases. The comparison of simulation and theoretical results proves the accuracy of the mathematical model.

Fig. 9 illustrates that network-level energy spectral efficiency is a function of user density/base station density. Given $B = 8$ MHz, user rates are divided into three cases. Fig. 9 proves the correctness of the above theoretical analysis. That is, there is a unique optimal value to maximize the network energy spectral efficiency. According to Fig. 9, when the user rate increases, the number of users that the network can accommodate will decrease to ensure optimal network energy spectrum efficiency. Because the increased user rate must be compensated by more base station deployments.

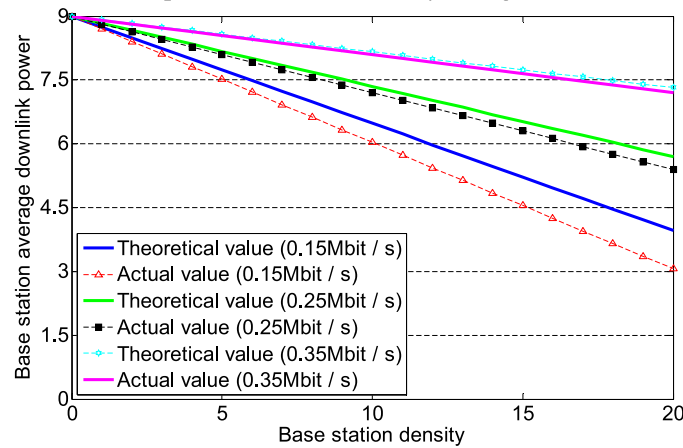
In Fig. 10, the static transmission power of a given base station is 40 W, and the system bandwidth is 18 MHz. The network area energy spectral efficiency is evaluated under different load distribution densities. The user density ranges from 0 to 4×10^{-4} users/m², which corresponds to 0 to 80 users/per cell. According to Fig. 10, it is found that the network power consumption of the base station deployment strategy based on high energy spectral efficiency load sensing is much lower than other related work. Moreover, the gap between the two increases as the user rate increases.

5. Conclusion

This paper focuses on the design of network architecture for information content transmission and distribution. Based on this, it studies the improvement of the communication performance of mobile nodes. In particular, it studies the relationship and impact of frequent switching of mobile nodes and the content-centric network architecture in high-speed mobile scenarios. Subsequently, a 5G mobile communication network architecture based on a content-centric network was



(a) The trend of the theoretical and simulation results of the base station's average downlink power as the user density changes



(b) The trend of the theoretical and simulation results of the base station's average downlink power as the base station density changes

Fig. 8. Trend of theoretical and simulation results of the average downlink power of the base station.

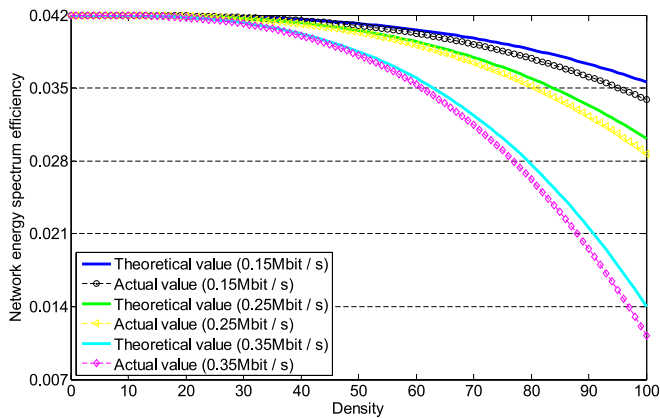


Fig. 9. Theoretical and simulated network energy spectral efficiency changes with user density/base station density.

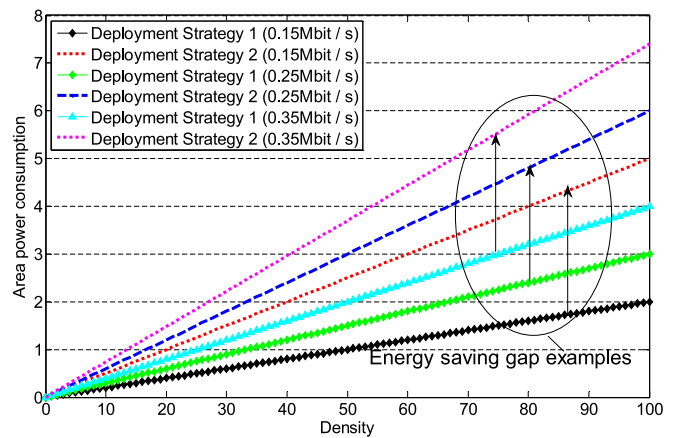


Fig. 10. Energy spectrum efficiency of network area under different deployment strategies.

proposed. Based on the core capability indicators required by 5G, research is conducted on the communication performance of the content-centric network-based 5G architecture. Aiming at the static deployment of cross-domain virtual network functions, a 5G cross-domain virtual network mapping method is proposed. It realizes the efficient division of cross-domain virtual networks, and can allocate and deploy resources

based on the characteristics of non-disclosure of information and different resource costs. The experimental simulation results show that this method can effectively reduce the resource overhead across multiple data domains with limited increase in running time. The problem of network energy spectrum efficiency optimization based on user basic

service quality constraints is presented. In different practical scenarios, the resource reduction gain of the strategy is evaluated. The simulation results show the accuracy of the mathematical model and verify the influence of different system parameters on the network energy spectrum efficiency. However, mathematical models and analysis results may not be completely applicable in practice. There is a difference between the spatial Poisson point distribution model in random geometry and the actual base station distribution. How to achieve a high degree of coincidence between theoretical, simulation and actual cellular scenes is the direction of future research.

CRedit authorship contribution statement

Zhiliang Liu: Formal analysis. **Zengzhi Zou:** Validation.

Declaration of competing interest

The authors declare that they have no known competing financial interests or personal relationships that could have appeared to influence the work reported in this paper.

References

- [1] M.H. Alsharif, R. Nordin, M.M. Shakir, et al., Small cells integration with the macro-cell under LTE cellular networks and potential extension for 5G, *J. Electr. Eng. Technol.* 14 (6) (2019) 2455–2465.
- [2] J. Qiu, D. Grace, G. Ding, et al., Air-ground heterogeneous networks for 5G and beyond via integrating high and low altitude platforms, *IEEE Wirel. Commun.* 26 (6) (2019) 140–148.
- [3] Y.J. Yu, T.Y. Hsieh, A.C. Pang, Millimeter-wave backhaul traffic minimization for CoMP over 5G cellular networks, *IEEE Trans. Veh. Technol.* 68 (4) (2019) 4003–4015.
- [4] Y. Zhai, T. Bao, L. Zhu, et al., Toward reinforcement-learning-based service deployment of 5G mobile edge computing with request-aware scheduling, *IEEE Wirel. Commun.* 27 (1) (2020) 84–91.
- [5] S. Guo, D. Zeng, L. Gu, et al., When green energy meets cloud radio access network: Joint optimization towards brown energy minimization, *Mob. Netw. Appl.* 24 (3) (2019) 962–970.
- [6] F. Zhou, W. Li, L. Meng, et al., Capacity enhancement for hotspot area in 5G cellular networks using mmwave aerial base station, *IEEE Wirel. Commun. Lett.* 8 (3) (2019) 677–680.
- [7] A. Mahmood, M.I. Ashraf, M. Gidlund, et al., Time synchronization in 5G wireless edge: Requirements and solutions for critical-MTC, *IEEE Commun. Mag.* 57 (12) (2019) 45–51.
- [8] D. Wang, B. Song, D. Chen, et al., Intelligent cognitive radio in 5G: AI-based hierarchical cognitive cellular networks, *IEEE Wirel. Commun.* 26 (3) (2019) 54–61.
- [9] K. Grochla, M. Slabicki, Transmit power optimisation in cellular networks with nomadic base stations, *IET Commun.* 13 (18) (2019) 3068–3074.
- [10] M.L. Attiah, A.A.M. Isa, Z. Zakaria, et al., Joint QoE-based user association and efficient cell-carrier distribution for enabling fully hybrid spectrum sharing approach in 5G mmWave cellular networks, *Wirel. Netw.* 25 (8) (2019) 5027–5043.
- [11] M. Taghavi, J. Abouei, Two-dimensional drone base station placement in cellular networks using MINLP model, *Int. J. Electron. Telecommun.* 65 (4) (2019) 701–706.
- [12] S. Zaidi, O.B. Smida, S. Affes, et al., User-centric base-station wireless access virtualization for future 5G networks, *IEEE Trans. Commun.* 67 (7) (2019) 5190–5202.
- [13] S.K. Tayyaba, M.A. Shah, Resource allocation in SDN based 5G cellular networks, *Peer-to-Peer Netw. Appl.* 12 (2) (2019) 514–538.
- [14] S. Andreev, V. Petrov, M. Dohler, et al., Future of ultra-dense networks beyond 5G: harnessing heterogeneous moving cells, *IEEE Commun. Mag.* 57 (6) (2019) 86–92.
- [15] G.R. MacCartney, T.S. Rappaport, Millimeter-wave base station diversity for 5G coordinated multipoint (CoMP) applications, *IEEE Trans. Wireless Commun.* 18 (7) (2019) 3395–3410.
- [16] Y. Hao, M. Chen, D. Cao, et al., Cognitive-caching: Cognitive wireless mobile caching by learning fine-grained caching-aware indicators, *IEEE Wirel. Commun.* 27 (1) (2020) 100–106.
- [17] A. Bonfante, L.G. Giordano, D. López-Pérez, et al., 5G massive MIMO architectures: Self-backhauled small cells versus direct access, *IEEE Trans. Veh. Technol.* 68 (10) (2019) 10003–10017.
- [18] J. He, W. Guan, W. Guo, et al., Analytical evaluation of cellular network uplink communications with higher order sectorization deployments, *IEEE Trans. Veh. Technol.* 68 (12) (2019) 12179–12189.
- [19] B.U. Kazi, G.A. Wainer, Next generation wireless cellular networks: ultra-dense multi-tier and multi-cell cooperation perspective, *Wirel. Netw.* 25 (4) (2019) 2041–2064.
- [20] J. Martín-Pérez, L. Cominardi, C.J. Bernardos, et al., Modeling mobile edge computing deployments for low latency multimedia services, *IEEE Trans. Broadcast.* 65 (2) (2019) 464–474.
- [21] J.S. Wey, J. Zhang, Passive optical networks for 5G transport: technology and standards, *J. Lightwave Technol.* 37 (12) (2018) 2830–2837.
- [22] H. Li, K. Ota, M. Dong, ECCN: Orchestration of edge-centric computing and content-centric networking in the 5G radio access network, *IEEE Wirel. Commun.* 25 (3) (2018) 88–93.
- [23] A. Martín, J. Egaña, J. Flórez, et al., Network resource allocation system for QoE-aware delivery of media services in 5G networks, *IEEE Trans. Broadcast.* 64 (2) (2018) 561–574.
- [24] J. Liu, Y. Shi, L. Zhao, et al., Joint placement of controllers and gateways in SDN-enabled 5G-satellite integrated network, *IEEE J. Sel. Areas Commun.* 36 (2) (2018) 221–232.